PTEP

Prog. Theor. Exp. Phys. **2013**, 00000 (8 pages)
DOI: 10.1093/ptep/0000000000

arXiv:1411.6708v1 [nucl-ex] 25 Nov 2014

Observation of the "K^-pp"-like structure in the $d(\pi^+, K^+)$ reaction at 1.69 GeV/c

Yudai Ichikawa[1,2], Tomofumi Nagae[1,*], Hiroyuki Fujioka[1], Hyoungchan Bhang[3], Stefania Bufalino[4], Hiroyuki Ekawa[1,2], Petr Evtoukhovitch[5], Alessandro Feliciello[4], Shoichi Hasegawa[2], Shuhei Hayakawa[6], Ryotaro Honda[7], Kenji Hosomi[2], Kenichi Imai[2], Shigeru Ishimoto[8], Changwoo Joo[3], Shunsuke Kanatsuki[1], Ryuta Kiuchi[2], Takeshi Koike[7], Harphool Kumawat[9], Yuki Matsumoto[7], Koji Miwa[7], Manabu Moritsu[10], Megumi Naruki[1], Masayuki Niiyama[1], Yuki Nozawa[1], Ryosuke Ota[6], Atsushi Sakaguchi[6], Hiroyuki Sako[2], Valentin Samoilov[5], Susumu Sato[2], Kotaro Shirotori[10], Hitoshi Sugimura[2], Shoji Suzuki[8], Toshiyuki Takahashi[8], Tomonori Takahashi[10], Hirokazu Tamura[7], Toshiyuki Tanaka[6], Kiyoshi Tanida[3], Atsushi Tokiyasu[10], Zviadi Tsamalaidze[5], Bidyut Roy[9], Mifuyu Ukai[7], Takeshi Yamamoto[7] and Seongbae Yang[3]

[1]*Department of Physics, Kyoto University, Kyoto 606-8502, Japan*
[2]*ASRC, Japan Atomic Energy Agency, Ibaraki 319-1195, Japan*
[3]*Department of Physics and Astronomy, Seoul National University, Seoul 151-747, Korea*
[4]*INFN, Istituto Nazionale di Fisica Nucleare, Sez. di Torino, I-10125 Torino, Italy*
[5]*Joint Institute for Nuclear Research, Dubna, Moscow Region 141980, Russia*
[6]*Department of Physics, Osaka University, Toyonaka 560-0043, Japan*
[7]*Department of Physics, Tohoku University, Sendai 980-8578, Japan*
[8]*High Energy Accelerator Research Organization (KEK), Tsukuba, 305-0801, Japan*
[9]*Nuclear Physics Division, Bhabha Atomic Research Centre, Mumbai, India*
[10]*Research Center for Nuclear Physics, Osaka University, Osaka 567-0047, Japan*
[*]*E-mail: nagae@scphys.kyoto-u.ac.jp*

We have observed a "K^-pp"-like structure in the $d(\pi^+, K^+)$ reaction at 1.69 GeV/c. In this reaction $\Lambda(1405)$ hyperon resonance is expected to be produced as a doorway to form the K^-pp through the $\Lambda^*p \to K^-pp$ process. However, most of the produced $\Lambda(1405)$'s would escape from deuteron without secondary reactions. Therefore, coincidence of high-momentum (> 250 MeV/c) proton(s) in large emission angles ($39^\circ < \theta_{lab.} < 122^\circ$) was requested to enhance the signal-to-background ratio. A broad enhancement in the proton coincidence spectra are observed around the missing-mass of 2.27 GeV/c^2, which corresponds to the K^-pp binding energy of 95 $^{+18}_{-17}$ (stat.) $^{+30}_{-21}$ (syst.) MeV and the width of 162 $^{+87}_{-45}$ (stat.) $^{+66}_{-78}$ (syst.) MeV.

Subject Index Kaonic nuclei, J-PARC

1. Introduction. Whether there exist kaonic nuclei or not is a key issue to make our understandings on the $\bar{K}N$ interaction in vacuum and in nuclear medium. The information on the $\bar{K}N$ interaction has been obtained by analyzing low-energy $\bar{K}N$ scattering data and kaonic-atom X-ray data [1]. The recent measurement of the energy shift and width on kaonic-hydrogen X-ray in high precision by the SIDDHARTA group [2] has contributed a lot [3]. From the theoretical analyses by using these results, it is well known that the $\bar{K}N$

© The Author(s) 2012. Published by Oxford University Press on behalf of the Physical Society of Japan.
This is an Open Access article distributed under the terms of the Creative Commons Attribution License (http://creativecommons.org/licenses/by-nc/3.0), which permits unrestricted use, distribution, and reproduction in any medium, provided the original work is properly cited.

interaction has a strong attraction in isospin 0 channel, which suggests possible existence of kaonic bound state formations [4]. Among them K^-pp bound state composed of a K^- and two protons could be the simplest one, if existed.

Since this is a three-body system, several groups (see a recent summary in [5] and [6–8]) calculated the binding energy and width of K^-pp by applying various few-body calculation techniques such as variational and Faddeev type calculations. The obtained binding energies are scattered in a broad range: 10–20 MeV for shallow potential cases and 50–100 MeV for deep cases. The width would be as wide as 70 MeV because of the strong $\bar{K}N$-$\pi\Sigma$ coupling. In addition there could be non-mesonic absorption contributions of $\bar{K}NN \to \Lambda(\Sigma)N$.

The first experimental evidence of the K^-pp bound state was reported by the FINUDA collaboration [9] in the stopped K^- absorption reactions on ^{6}Li, ^{7}Li, and ^{12}C targets. They observed a lot of Λp pairs emitted in back-to-back, and found the invariant mass of the pair significantly lower than K^-pp mass threshold. The binding energy of 115 $^{+6}_{-5}$ (stat.) $^{+3}_{-4}$ (syst.) MeV and the decay width of $\Gamma = 67$ $^{+14}_{-11}$ (stat.) $^{+2}_{-3}$ (syst.) MeV were obtained. However, there was a theoretical criticism [10] to interpret the observed structure as the K^-pp bound state.

Another experimental evidence was reported by the DISTO collaboration [11]. They measured the missng-mass and invariant mass spectra in an exclusive reactions of $pp \to K^+\Lambda p$ at 2.85 GeV. The binding energy of 103 $\pm$ 3 (stat.) $\pm$ 5(syst.) MeV and the width of 118 $\pm$ 8(stat.) $\pm$ 10(syst.) MeV were obtained. However, they did not observe the signal at 2.50 GeV [12], maybe due to the less production cross section of $\Lambda(1405)$ at this energy.

There is also a report of a narrow and much deeper binding for the K^-pp system observed in $\bar{p}$-^{4}He annihilations at rest [13]. No peak was observed in the inclusive spectrum of the $\gamma d \to K^+\pi^- X$ reaction at $E_\gamma = 1.5$–2.4 GeV [14].

Thus, the experimental situation for the K^-pp bound state is not conclusive at this moment. It would be important to obtain new experimental information in different reactions. In the J-PARC E27 experiment, we used the $d(\pi^+, K^+)$ reaction at 1.69 GeV/c to produce the K^-pp system through the $\Lambda(1405)$ production as a doorway [15]. This is a simple production measurement with the smallest final state effects.

2. Experimental Setup. The experiment was carried out at K1.8 beam line [16] of the hadron experimental hall at J-PARC [17]. In this beam line, separated $K^\pm, \pi^\pm, p$, and $\bar{p}$ beams up to 2 GeV/c are delivered. The detail of the experimental setup of this measurement are described in Ref. [18, 19].

The beam line is equipped with a beam line spectrometer for the incident π^+ momentum reconstruction composed of four quadrupole magnets and one dipole magnet. The out-going K^+ momentum was reconstructed with the Superconducting Kaon Spectrometer (SKS) with the momentum resolution of $\Delta p/p \sim 1 \times 10^{-3}$.

A liquid hydrogen/deuterium target was installed 1.3 m upstream from the entrance of the SKS magnet, so that the solid angle acceptance of the SKS was about 100 msr. The size of the target cell was 120 mm in length and 67.3 mm in diameter, which contains 1.99 g/cm^2 of liquid deuterium.

2.1. Range Counter Arrays. In order to suppress a large backgrounds coming from quasi-free productions of hyperons (Λ and Σ's) and hyperon resonances ($\Lambda(1405)$ and $\Sigma(1385)$'s), a

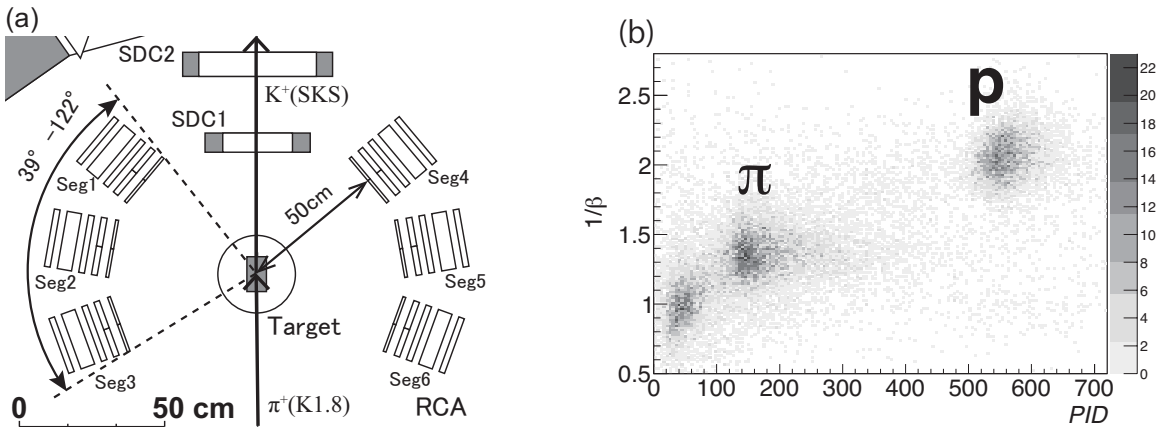

Fig. 1 (a) Schematic view of the range counter system. It was composed of six range counter arrays; three in the left (Seg1 to Seg3) and three in the right (Seg4 to Seg6) of the beam axis. SDC1 and 2 were the tracking drift chamber at the entrance of the SKS. (b) A scatter plot between the PID function and $1/\beta$. Protons are clearly separated from pions.

range counter system was installed surrounding the liquid deuterium target in the laboratory angles between 39° and 122° both in the left and right sides from the beam axis as shown in Fig. 1 (a). We had three range counter arrays (RCA's) in each side and the assignment of the segment number is also shown in Fig. 1 (a).

Each range counter array had five layers of plastic scintillation counters; the thickness of each scintillator was 1 cm, 2 cm, 2 cm, 5 cm, and 2 cm, respectively, with a height of 100 cm. The width of each layer was 20 cm. The first two layers were segmented into two slabs; each slab had 10-cm width. Therefore, we had seven (2+2+1+1+1) scintillation counters in one range counter array. Every scintillation counter was read out from both sides (up and down) by photo-multiplier tubes (PMT).

From each PMT, both hit timing and pulse height information were obtained. The discriminator threshold for the timing information was set at less than the one tenth level of the minimum ionizing particles. The timing information from the first layer was used for the on-line trigger and the time-of-flight analysis in off-line. The distance from the liquid target center to the first layer was about 50 cm. In the on-line trigger, the (π, K) trigger in coincidence with range counter hits was generated by requiring at least one hit among 12 first-layer scintillators.

From a hit pattern of five layers, we can define the stopping layer, i_{stop}, for each range counter array. Then, we set up a particle identification parameter, PID, as,

$$PID = (dE_{i_{stop}} + dE_{(i_{stop}-1)})^{\alpha} - (dE_{i_{stop}})^{\alpha}, \tag{1}$$

where dE_i shows the energy deposit in the i-th layer of the plastic scintillators. The PID is a function of particle mass when the parameter $\alpha(\sim 1.75)$ is properly adjusted.

The time-of-flight (TOF) of each particle was obtained with the hit timing in the first layer. The flight path length was measured from the vertex position of the (π^+, K^+) reaction to the hit position on the first layer. In this analysis, the horizontal hit position was assumed to be the center of the scintillators and the vertical hit position was obtained with the time difference between the up and down PMT's. Then, the velocity of the particle (β) was obtained as $\beta = (\text{path length})/(\text{TOF}\cdot c)$, which was adjusted by using the π^+ of $\beta \sim 1$.

Thus, we used the PID function and the velocity (β) for the particle identification between proton and pion. Fig. 1 (b) shows an example of a scatter plot between PID and $1/\beta$ in the case of $i_{stop} = 4$ in one of the RCA. In this analysis, the proton was selected as the gate of $\pm 3\sigma$ in PID and $\pm 2\sigma$ in $1/\beta$ for each stopping layer. Protons are clearly separated from pions. The energy of proton was determined from the velocity.

From a study of the hydrogen target data, we could identify the proton from the Σ^+ decay ($\Sigma^+ \to p\pi^0$) with a detection efficiency of 65 % for protons hitting the first layer of RCA. The detection efficiency was limited due to a leakage of particles at the side edges of RCA.

3. Inclusive and Coincidence Analyses. Fig. 2 (a) shows the inclusive missing-mass (MM_d) spectrum for the $\pi^+ d \to K^+ X$ reaction at 1.69 GeV/c in the scattering angles between 2° and 14° in the laboratory frame, which is a spectrum without acceptance correction. The overall missing-mass resolution was estimated from the missing-mass spectra of $\pi^+ p \to K^+ \Sigma^+$ reactions at 1.58 GeV/c and 1.69 GeV/c, and it was 2.8 ± 0.1 MeV/c^2 (FWHM). The details of the inclusive analyses were reported in Ref. [19].

As shown in Fig. 2 (a), the missing-mass spectrum is composed of three major components: I) the quasi-free $\pi^+ n \to K^+ \Lambda$ contribution (QFΛ), II) the quasi-free $\pi^+ p \to K^+ \Sigma^+$ and $\pi^+ n \to K^+ \Sigma^0$ contributions (QFΣ), and III) a mixture of the quasi-free $\pi^+ N \to K^+ \Sigma(1385)$, $\pi^+ n \to K^+ \Lambda(1405)$ (QFY^*), and $\pi^+ N \to K^+ (\Lambda/\Sigma)\pi$ (QF$Y\pi$). In between the QFΛ and QFΣ, we have a small peculiar structure corresponding to a threshold cusp for the $\Sigma N \to \Lambda N$ conversion process.

Next, we request coincidence of one proton. According to our detector simulation, a proton emitted from QFΛ, QFΣ, QFY^*, and QF$Y\pi$ processes rarely hits the RCA; only small fraction in the very forward segments (Seg1, 4). The spectator proton in a deuteron rarely exceeds the analysis threshold momentum of 250 MeV/c. Therefore, we can expect a good suppression of the quasi-free processes in one-proton coincidence spectrum.

Fig. 2 (b) shows a coincidence spectrum with one proton in the middle segments of the RCA in each side (Seg2, 5), where these segments have an almost flat and wide acceptance in missing mass. Note that there would be no quasi-free contributions in this spectrum according to the simulation. Possible non-quasifree contributions are the threshold cusp emitting through a strong conversion of $\Sigma^+ n \to \Lambda p$, the $K^- pp$ signal emitting through $K^- pp \to \Lambda(\Sigma^0)p$, and quasi-free hyperons and hyperon resonance productions followed by conversions such as $\Sigma N \to \Lambda N$.

In Fig. 2 (c), we present a ratio histogram between the one-proton coincidence spectrum (Fig. 2 (b)) and the inclusive one (Fig. 2 (a)). This is a spectrum without acceptance correction for the RCA. The vertical axis shows the proton coincidence probability as a function of the missing mass. The background contamination from the miss-identification of $\pi^{+/-}$ in RCA, which is estimated by the side-band events in PID, is shown with hatched spectra in Figs. 2 (b) and (c). The contamination fraction of this background is about 7% around $\mathrm{MM}_d \sim 2.27$ GeV/c^2.

We notice there are two prominent structures; one at the threshold cusp position (2.13 GeV/c^2) and the other broad bump at around 2.27 GeV/c^2, which can be a signal of the "$K^- pp$"-like structure. In the QFΣ and QFY^* region, the proton coincidence probability is smaller than the two prominent structures and stays rather constant.

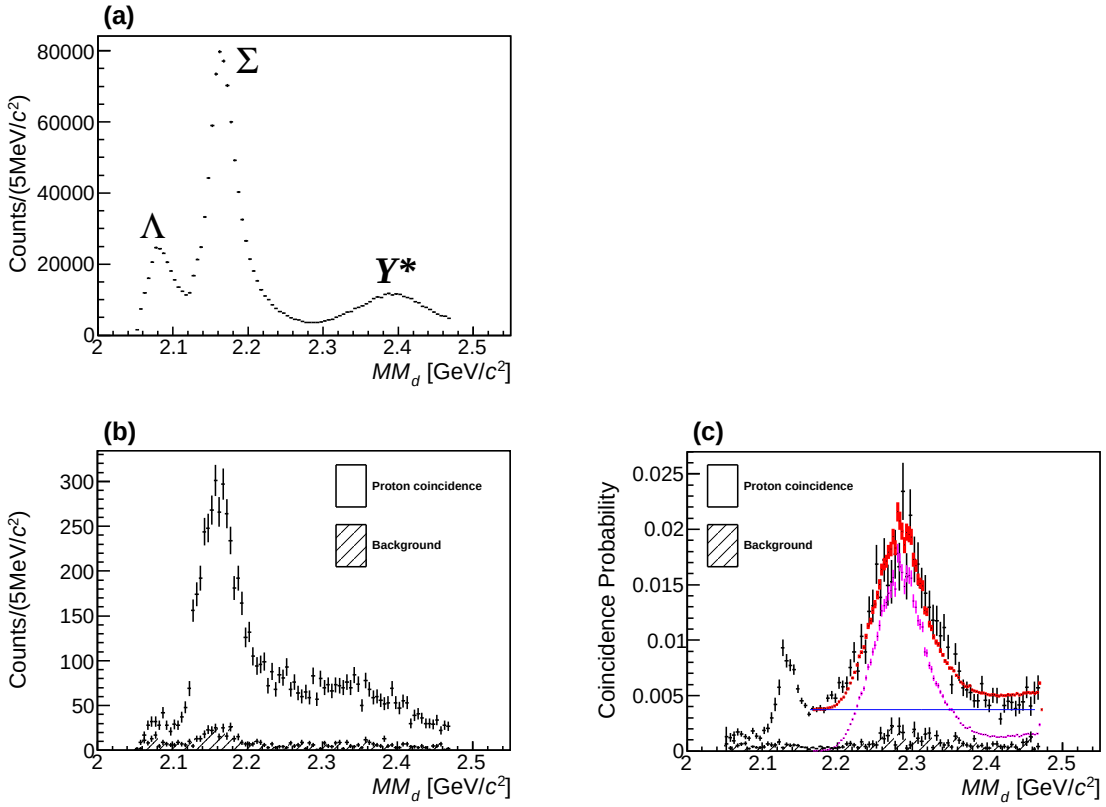

Fig. 2 (a) Inclusive missing-mass spectrum of the $d(\pi^+, K^+)$ reaction at 1.69 GeV/c in the laboratory scattering angles from 2° to 14°. (b) Missing-mass spectrum of the $d(\pi^+, K^+)$ reaction with one proton in the middle of the RCA in each side (Seg2, 5). (c) The coincidence probability of a proton obtained by dividing the coincidence spectrum (b) with the inclusive spectrum (a). Hatched spectra show the background contamination from the miss-identification of $\pi^\pm$ in RCA. See the text in page 7 for the detail of colored spectra in (c).

At this stage, the acceptance of our range counter system is not taken into account. The acceptance correction needs information of decay modes of the "K^-pp"-like structure. This study was carried out by requiring coincidence of two protons in the RCA's. In such a condition, we can measure the missing-mass of X in the $d(\pi^+, K^+pp)X$ process by detecting two protons in the decay of the ppX system, of which mass is MM_d, in three categories; a) Λp, $\Lambda \to p\pi^-$, b) $\Sigma^0 p$, $\Sigma^0 \to \Lambda\gamma \to p\pi^-\gamma$, and c) $Y\pi\mathrm{N} \to pp\pi\pi$. The first two modes, a) and b), are non-mesonic and the X is one pion (and γ). The last one, c), is mesonic and the X is two pions. Therefore, the missing-mass spectrum of M_X should show different distributions for each decay mode. Fig. 3 shows such missing-mass square spectra of M_X. Three distributions estimated for each decay mode are shown in the figure by fitting the height of each template distribution. These templates were made from the simulation, which assumes the reaction of $\pi^+ d \to K^+ W, W \to pY(p(Y\pi))$ with uniform productions and decays in the center of mass system.

According to these fitting results, we can correct the acceptance of the RCA for each decay mode. It is almost flat in the missing mass except near the threshold for each decay mode. Fig. 4 shows a missing-mass distribution for two-protons coincidence events of the Σ^0p final state b) with the acceptance correction. The spectrum was fitted with a relativistic

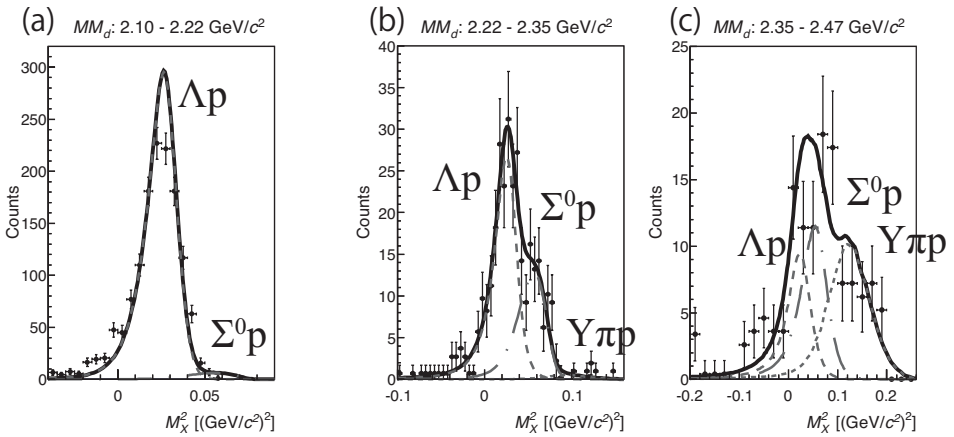

Fig. 3 Missing-mass square spectra of X obtained in the two-protons coincidence events in the reaction of the $d(\pi^+, K^+pp)X$. Each spectrum shows the mass square of X for different MM_d region; the left (a) shows the QFΣ region ($MM_d < 2.22$ GeV/c^2), the center (b) shows "K^-pp"-like structure region ($2.22 < MM_d < 2.35$ GeV/c^2) and the right (c) shows the QFY^* region ($MM_d > 2.35$ GeV/c^2). The spectra were fitted with three components of Λp (dashed line), $\Sigma^0 p$ (dot-dashed line) and $Y\pi p$ (dotted line) decay modes.

Breit-Wigner function as,

$$f(MM_d) = \frac{(2/\pi)MM_d m_0 \Gamma(q)}{(m_0^2 - MM_d^2)^2 + (m_0\Gamma(q))^2}. \tag{2}$$

The mass-dependent width was $\Gamma(q) = \Gamma_0(q/q_0)$, in which q (q_0) is the momentum of the Σ^0 and proton in the $\Sigma^0 p$ rest frame at mass MM_d (m_0). The obtained mass and width are 2275 $^{+17}_{-18}$ (stat.) $^{+21}_{-30}$ (syst.) MeV/c^2 and 162 $^{+87}_{-45}$ (stat.) $^{+66}_{-78}$ (syst.) MeV, respectively. It corresponds to the biding energy of the K^-pp system to be 95 $^{+18}_{-17}$ (stat.) $^{+30}_{-21}$ (syst.) MeV and the production cross section of the "K^-pp"-like structure decaying to $\Sigma^0 p$ of $d\sigma/d\Omega_{K^-pp\to\Sigma^0 p}$ $= 4.4 \pm 0.4$ (stat.) $^{+0.8}_{-1.6}$ (syst.) $\mu b/sr$. The systematic errors of these values were estimated taking into account uncertainties in the fitting ranges, the binning of the missing-mass spectrum, the detection efficiency of two protons in RCA and the Breit-Wigner shape by changing the Lorentzian function folded with the missing-mass resolution. The differential cross section of "K^-pp"-like structure of the Λp decay mode a) was also estimated from the fitting assuming the same distribution of MM_d. Thus, a branching fraction of the "K^-pp"-like structure was obtained to be $\Gamma_{\Lambda p}/\Gamma_{\Sigma^0 p} = 0.73$ $^{+0.13}_{-0.11}$ (stat.) $^{+0.43}_{-0.21}$ (syst.). This ratio was discussed from a theoretical point in Ref. [20].

Next, we try to understand the ratio histogram (Fig. 2 (c)) with the obtained K^-pp mass distribution of $f(MM_d)$. By using the mass distribution for the "K^-pp"-like structure and the double differential cross section of the inclusive (π^+, K^+) process $\frac{d^2\sigma}{d\Omega dMM_d}(MM_d)_{Inclusive}$, we can obtain the ratio histogram as shown in Fig. 2 (c) as a plot colored in pink, which is calculated as,

$$R_p(MM_d) = \frac{C \times f(MM_d) \times \eta_{1p}(MM_d)}{(\frac{d^2\sigma}{d\Omega dMM_d}(MM_d))_{Inclusvie}}, \tag{3}$$

where C is the normalization constant, and $\eta_{1p}(MM_d)$ is the detection efficiency of a proton in the middle segments of the RCA (Seg2, 5). A blue line in Fig. 2 (c) is an assumed flat component representing the conversion processes and the background contamination from

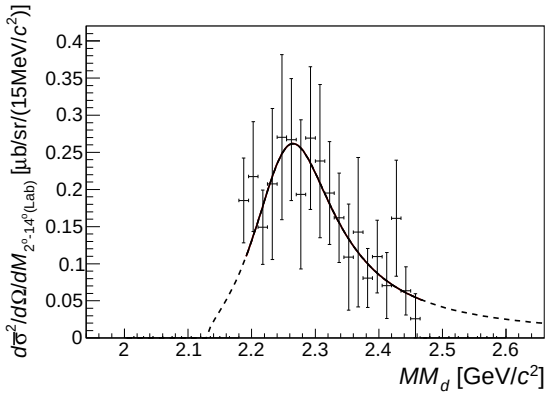

Fig. 4 Missing-mass spectrum of the $d(\pi^+, K^+)$ reaction for two-protons coincidence and the $\Sigma^0 p$ decay branch events. The mass acceptance of the RCA's are corrected. The spectrum was fitted with a relativistic Breit-Wigner function (see the text for the detail). We found the mass 2275 $^{+17}_{-18}$ (stat.) $^{+21}_{-30}$ (syst.) MeV/c^2 and the width 162 $^{+87}_{-45}$ (stat.) $^{+66}_{-78}$ (syst.) MeV.

the miss-identification of $\pi^{\pm}$ in RCA. Red points with error bars in Fig. 2 (c) are the sum of the pink points and blue line. The normalization constant C and the amplitude of the flat component (blue line) were adjusted to minimize the differences between the black and red points. Thus, the obtained one proton coincidence probability spectrum of the broad enhanced region could be reproduced by the "K^-pp" and flat background.

What is the nature of the "K^-pp-like structure? It should have strangeness -1 and baryon number $B = 2$ from the observed reaction mode, so that the hyper charge $Y = 1$. As for the spin of the K^-pp system, a K^- is theoretically assumed to couple with a spin-singlet ($S = 0$) p-p pair in S-wave ($L = 0$). So that the $J^P = 0^-$, presumably. Alternative view of the system as a $\Lambda^* p$ bound state [21] also predicts the bound state spin to be 0. There is also a theoretical prediction of a $(Y, I, J^P) = (1, 3/2, 2^+)$ dibaryon as $\pi\Lambda N$–$\pi\Sigma N$ bound state [22].

4. Summary. We have observed a "K^-pp"-like structure in the $d(\pi^+, K^+)$ reaction at 1.69 GeV/c with coincidence of high-momentum (>250 MeV/c) proton(s) in large emission angles ($39^\circ < \theta_{lab.} < 122^\circ$). A broad enhancement in the proton(s) coincidence spectra are observed around the missing-mass of 2.27 GeV/c^2, which corresponds to the binding energy of the K^-pp system of 95 $^{+18}_{-17}$ (stat.) $^{+30}_{-21}$ (syst.) MeV and the width of 162 $^{+87}_{-45}$ (stat.) $^{+66}_{-78}$ (syst.) MeV. The branching fraction between the Λp and $\Sigma^0 p$ decay modes of the "K^-pp"-like structure was measured to be $\Gamma_{\Lambda p}/\Gamma_{\Sigma^0 p} = 0.73$ $^{+0.13}_{-0.11}$ (stat.) $^{+0.43}_{-0.21}$ (syst.), for the first time.

Acknowledgements

We would like to thank the Hadron beam channel group, accelerator group and cryogenics section in J-PARC for their great efforts on stable machine operation and beam quality improvements. The authors thank the support of NII for SINET4. This work was supported by the Grant-In-Aid for Scientific Research on Priority Area No. 449 (No. 17070005), the Grant-In-Aid for Scientific Research on Innovative Area No. 2104 (No. 22105506), from the Ministry of Education, Culture, Sports, Science and Technology (MEXT) Japan, and Basic Research (Young Researcher) No. 2010-0004752 from National Research Foundation in Korea. We thank supports from National Research Foundation, WCU program of the Ministry of Education, Science and Technology (Korea), Center for Korean J-PARC Users.

References

[1] A.D. Martin, References included in the following theoretical analyses, Nucl. Phys. B **179**, 33 (1981); N. Kaiser, P.B. Siegel and W. Weise, Nucl. Phys. **A594**, 325 (1995).
[2] M. Bazzi et al., Phys. Lett. **B704**, 113 (2011); M. Bazzi et al., Nucl. Phys. A **881**, 88 (2012).
[3] T. Hyodo, Nucl. Phys. A **914**, 259 (2013).
[4] Y. Akaishi and T. Yamazaki, Phys. Rev. C **65**, 044005 (2002); T. Yamazaki and Y. Akaishi, Phys. Lett. **B535**, 70 (2002).
[5] A. Gal, Nucl. Phys. A **914**, 270 (2013), particularly Table 1.
[6] S. Maeda, Y. Akaishi, T. Yamazaki, Proc. Jpn. Acad. B **89**, 418 (2013).
[7] M. Bayar and E. Oset, Phys. Rev. C **88**, 044003 (2013).
[8] J. Révai and N.V. Shevchenko, Phys. Rev. C **90**, 034004 (2014).
[9] M. Agnello et al., Phys. Rev. Lett. **94**, 212303 (2005).
[10] V.K. Magas, E. Oset, A. Ramos, and H. Toki, Phys. Rev. C **74**, 025206 (2006); A. Ramos, V. K. Magas, E. Oset, and H. Toki, Nucl. Phys. A **804**, 219 (2008); V.K. Magas, E. Oset, and A. Ramos, Phys. Rev. C **77**, 065210 (2008).
[11] T. Yamazaki et al., Phys. Rev. Lett. **104**, 132502 (2010).
[12] P. Kienle et al., Euro. Phys. J. A **48**, 183 (2012).
[13] T.G. Bendiscioli et al., Euro. Phys. J. A **40**, 11 (2009); T.G. Bendiscioli et al., Nucl. Phys. A **789**, 222 (2007).
[14] A.O. Tokiyasu et al., Phys. Lett. **B728**, 616 (2012).
[15] T. Yamazaki and Y. Akaishi, Phys. Rev. C **76**, 045201 (2007).
[16] T. Takahashi et al., Prog. Theor. Exp. Phys. **2012**, 02B010 (2012).
[17] S. Nagamiya, Prog. Theor. Exp. Phys. **2012**, 02B001 (2012).
[18] Y. Ichikawa et al., presentation at "The 2nd International Symposium on Science at J-PARC 2014", Tsukuba July 2014. The proceedings will be published in JPS Conference Proceedings.
[19] Y. Ichikawa et al., Prog. Theor. Exp. Phys. **2014**, 101D03 (2014).
[20] T. Sekihara, D. Jido and Y, Kanada-En'yo, Phys. Rev. C **79**, 062201(R) (2009).
[21] T. Uchino, T. Hyodo and M. Oka, Nucl. Phys. A **868**, 53 (2011).
[22] H. Garcilazo and A. Gal, Nucl. Phys. A **897**, 167 (2013).